Zeitschrift: IABSE publications = Mémoires AIPC = IVBH Abhandlungen
Band: 31 (1971)

Artikel: A finite difference approach to corrugated shear panels
Autor: Horne, M.R. / Raslan, R.A.S.
DOI: https://doi.org/10.5169/seals-24209

A Finite Difference Approach to Corrugated Shear Panels

Méthode approchée des différences finies pour le calcul de panneaux à nervures

Eine endliche Differenz-Näherung für gerippte Schubfelder

M. R. HORNE
M. A., M. Sc., Ph. D., Sc. D.
Professor of Civil Engineering

R. A. S. RASLAN
B. Sc., Ph. D.

University of Manchester, England

1. Introduction

In the previous paper [1], the authors have summarised solutions which have been given by a number of workers [2, 3, 4, 5, 6, 7] to the problem of shear deformation of corrugated panels. The panel (Fig. 1) is assumed to be surrounded by rigid members which can themselves deform without resistance into a parallelogram, but restrain the panel against deformation out of its plane along all four edges. When a panel with trapezoidal corrugations is subjected

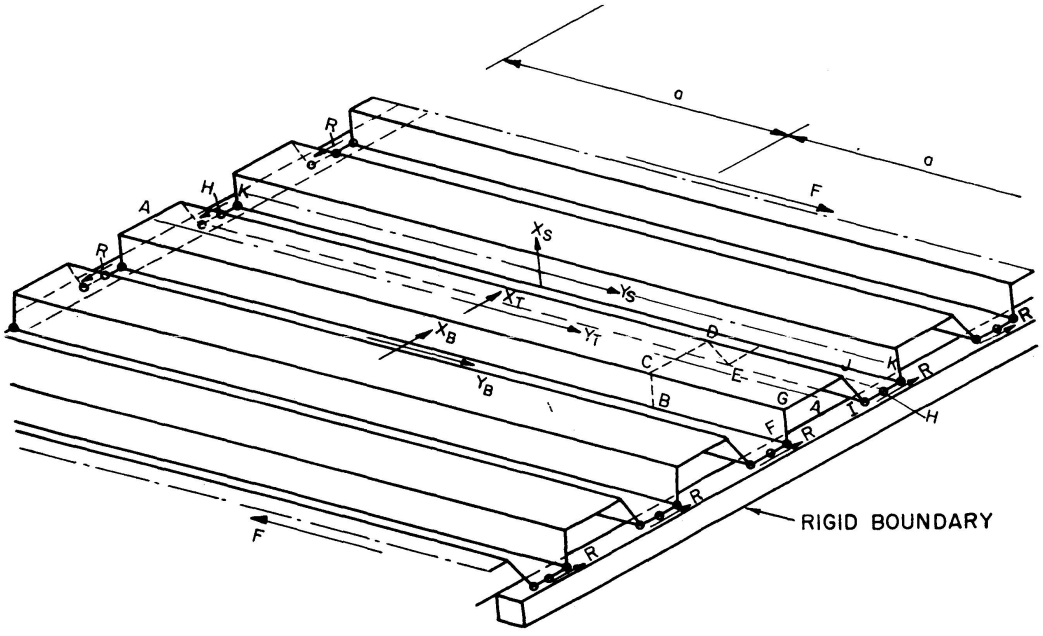

Fig. 1.

to a shear force F as shown in Fig. 1, the corrugations twist and deform as shown for a typical cross-section in Fig. 2. The bending stresses acting in the plane of Fig. 2 are an important feature of the stress pattern induced, and this bending may be referred to as "portal frame bending". The contribution to the stiffness of the panel of other bending stresses (bending stresses perpendicular to the plane of Fig. 2 and torsional bending stresses) are negligible because of the relatively low curvatures involved (low values of $\frac{\partial^2 w}{\partial y^2}$ and $\frac{\partial^2 w}{\partial x \partial y}$ compared with $\frac{\partial^2 w}{\partial x^2}$ where the y axis is parallel to the corrugations).

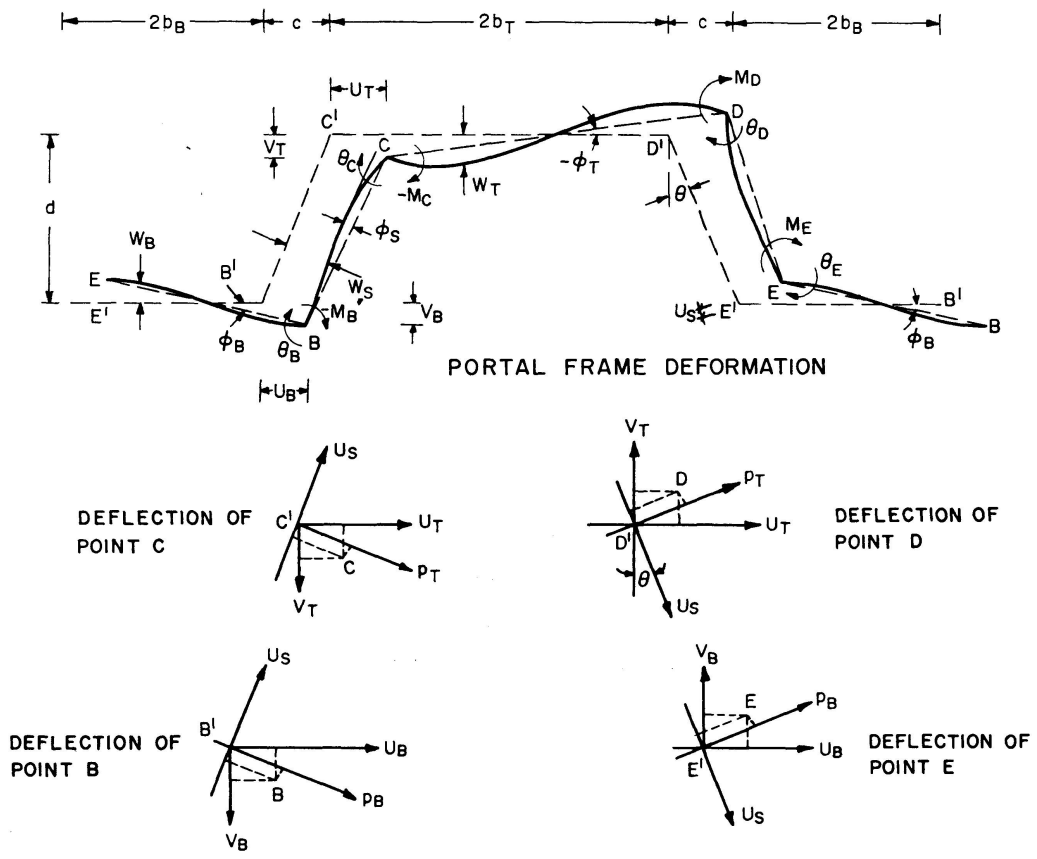

Fig. 2.

The other stresses that have to be considered are the membrane stress components σ_x, σ_y and τ_{xy}. The normal stresses σ_x (acting perpendicular to the bent edges of the corrugations) are small because of the flexibility of the corrugations in this direction due to "portal frame bending", and the strains caused by stresses σ_x may be neglected.

The deflection pattern of the corrugated panel may be described by referring to the shape of the longitudinal centre line of each top, bottom and side plate (e. g. lines AA, HH and KK in Fig. 1). When the panel length 2a is very short, these remain straight when viewed perpendicular to the plane of the panel, the centre lines of the top plates undergoing a twist while those of the bottom

panels remain undeflected. In long panels all the centre lines become curved. The authors [1], by assuming simple sinusoidal shapes for the centre lines, have obtained expressions for the strain energy of the system, and by minimising the strain energy for a given shear displacement, have obtained a solution for the stiffness of the panel.

The limitation of this method of solution lies in the difficulty of describing the deflected shape of the centre lines when the real shape departs significantly from simple sinusoidal. In very long panels, the curvatures are small except near the ends, and an adequate description of the shape necessitates taking a number of terms in the Fourier series. Because of the complexity of the expressions this becomes an impracticable method of solution.

Instead of adopting assumed deflected forms, an equilibrium solution may be achieved by treating the top, bottom and side plates as prismatic beams bending in the planes of the respective plates. The equilibrium conditions are then solved by considering the bending, normal and shear forces acting within and between these prismatic beams, as shown in Fig. 4. Together with these

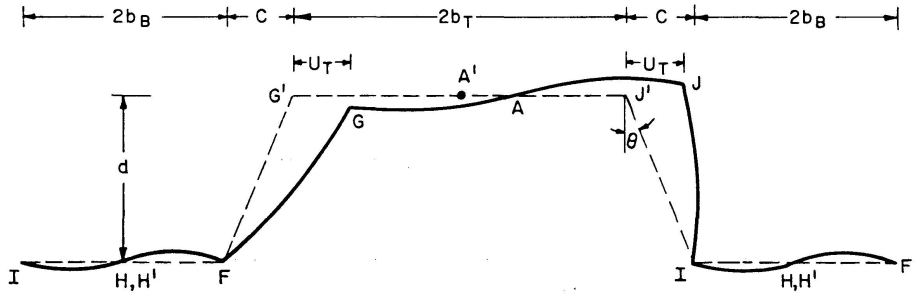

Fig. 3. Portal Frame Deformations at End of Panel.

forces are associated those due to the "portal frame bending" of the corrugations (Fig. 2), and the resulting equilibrium equations, when combined with the necessary compatibility conditions lead to a set of three simultaneous, linear fourth order differential equations which may be solved by finite difference methods.

2. The Force System in the Top, Bottom and Side Plates

The forces existing on elements of length dy along the length of a corrugation for top and side plates are shown in Fig. 4.

On an element of the top plate, the forces are

a) a normal edge force $p_T\,dy$ arising as a result of the portal frame bending;
b) shear forces F_T and F_T+dF_T in direction $0X$ and $Q_T\,dy$ in direction $0Y$, and
c) beam type bending moments M_T and M_T+dM_T.

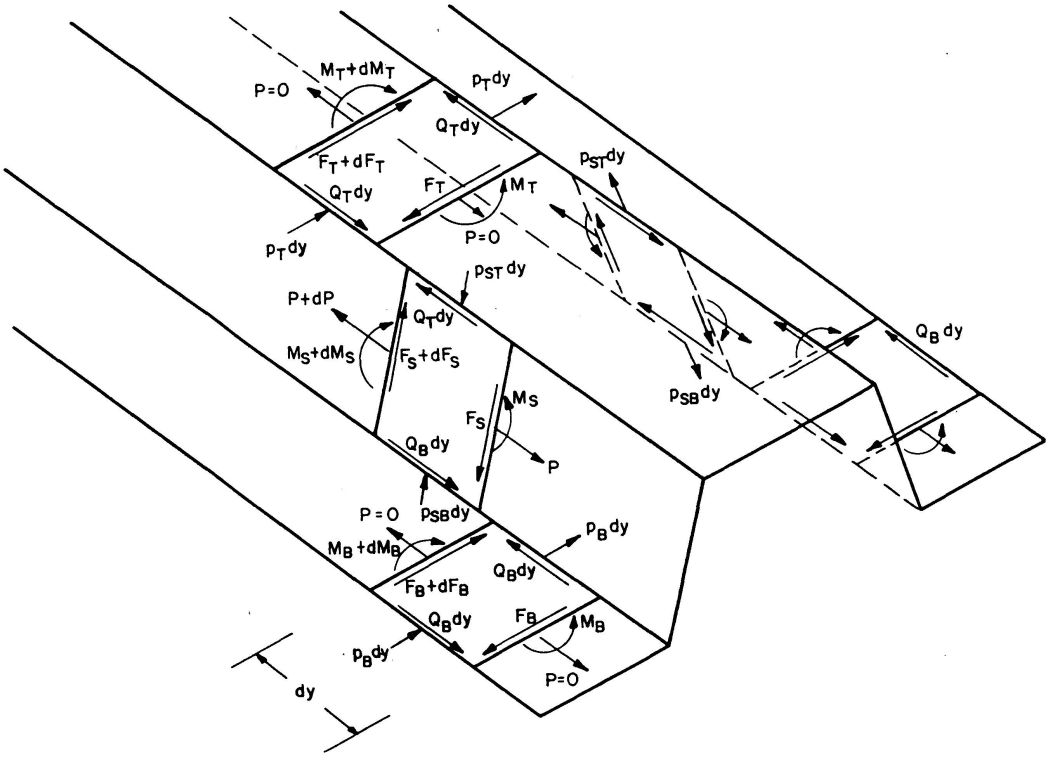

Fig. 4. Internal Forces.

Similarly on an element of the bottom plate, the forces are

a) a normal edge force $p_B\,dy$;
b) shear forces F_B and F_B+dF_B in direction $0X$ and $Q_B\,dy$ in direction $0Y$, and
c) beam type bending moments M_B and M_B+dM_B.

On an element of the side plate, the forces are

a) normal edge forces $p_{ST}\,dy$ and $p_{SB}\,dy$, giving a net force $(p_{ST}-p_{SB})\,dy$;
b) shear forces F_S and F_S+dF_S in direction $0X$ and $Q_T\,dy$ and $Q_B\,dy$ in direction $0Y$. Due to the difference in value between the shear forces on the two edges, mean normal forces P and $P+dP$ must also exist to maintain equilibrium, and finally;
c) beam type bending moments M_S and M_S+dM_S.

The equilibrium conditions between the external and internal forces require that

$$F_T+F_B+2\,F_S\sin\theta = R$$

and

$$\int_{-a}^{a} Q_T\,dy = \int_{-a}^{a} Q_B\,dy = \int_{-a}^{a} (Q_T-Q_B)\,dy+dP = F,$$

where F is the total applied shear force acting on the panel and R is the force at the end of each corrugation as shown by Fig. 1.

3. Assumptions

These are similar to those made in the energy solution [1], and are as follows:

1. The material is infinitely elastic.
2. The marginal frame is a hinged parallelogram of rigid members.
3. The plate is held to the frame at one point in the mid-width of each bottom plate in such a way that at its ends, the bottom plate is allowed to rotate in plan but is prevented from twisting about its longitudinal axis. Hence the deformed shape of the corrugation at its ends is as shown in Fig. 3.
4. No slip takes place due to bearing between the plate and the fasteners.
5. No local or overall buckling takes place.
6. The panel is very wide, that is, it consists of a large number of corrugations. This means that the behaviour of successive corrugations is identical.
7. The effect of large deformations is ignored.
8. The top plate is assumed to deflect freely, at its ends, so that $(F_T)_{y=a} = (M_T)_{y=a} = 0$.
9. The bottom and the side plates are hinged at their ends so that $(M_S)_{y=a} = (M_B)_{y=a} = 0$.

Moreover, using the notation for deflections given in Fig. 2, $(u_S)_{y=a} = (u_B)_{y=a} = 0$.

4. The Analysis of Portal Frame Bending

The deformed shape of a shear corrugated plate at any point along its length is demonstrated in Fig. 2, u_T, u_B, u_S being the in-plane deflections in the direction of the top, bottom and side plates respectively.

Expressions for bending moments $M_B = -M_E$ and $M_C = -M_D$ may be derived [1, 8] in terms of the in-plane deflections and the dimensions of the corrugation. These are:

$$M_B = \frac{D}{b_S^2 F}[J(u_T - u_B) + G u_S - G_1(u_T + u_B)], \tag{1}$$

$$M_C = \frac{-D}{b_S^2 F}[K(u_T - u_B) - H u_S + H_1 u_T + u_B)], \tag{2}$$

where $D = \frac{E t^3}{12(1-\mu^2)}$ is the flexural rigidity of the plate, t is the thickness, E the elastic modulus and μ Poisson's ratio and

$$\begin{aligned} F &= \frac{1}{3}\left[\left(2+\frac{b_B}{b_S}\right)\left(2+\frac{b_T}{b_S}\right)-1\right], \\ J &= \frac{b_S}{d}\left[3+\frac{b_T}{b_S}+\frac{c}{2b_S}\left(\frac{2b_S+b_T}{b_B}+\frac{b_S}{b_T}\right)\right], \end{aligned} \tag{3}$$

$$
\begin{aligned}
K &= \frac{b_S}{d}\left[3+\frac{b_B}{b_S}+\frac{c}{2b_S}\left(\frac{2b_S+b_B}{b_T}+\frac{b_S}{b_B}\right)\right],\\
G &= \frac{2b_S}{d}\left[\frac{2b_S+b_T}{b_B}-\frac{b_S}{b_T}\right],\\
H &= \frac{2b_S}{d}\left[\frac{2b_S+b_B}{b_T}-\frac{b_S}{b_B}\right],\\
G_1 &= \frac{G}{4}\,\frac{c}{b_S},\\
H_1 &= \frac{H}{4}\,\frac{c}{b_S}.
\end{aligned}
\tag{3}
$$

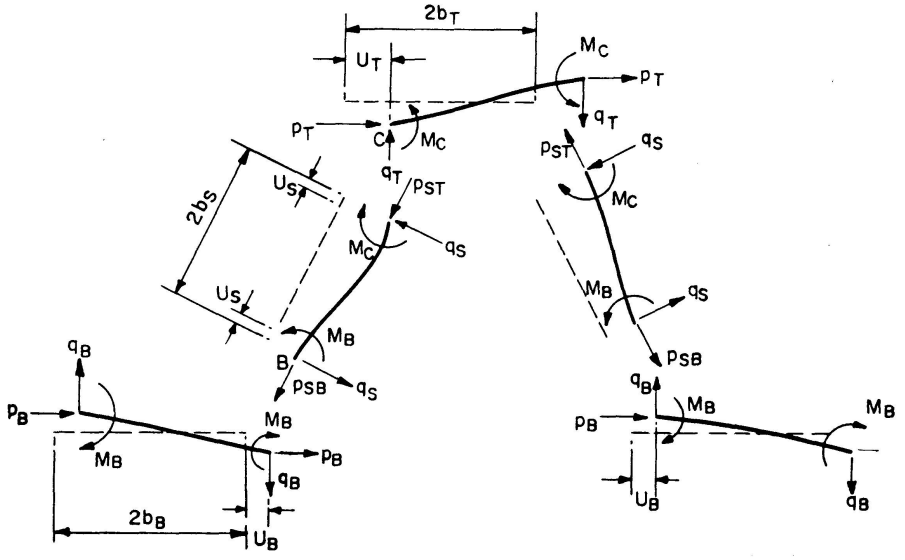

a) Force Frame Forces.

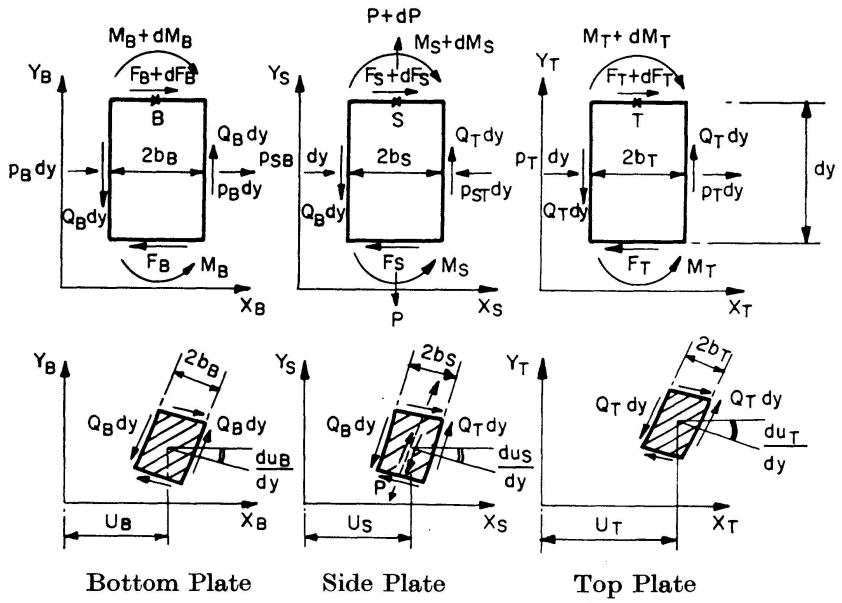

Bottom Plate Side Plate Top Plate

b) Forces and Displacements of Elements.

Fig. 5.

The dimensions b_T, b_B and b_S represent half the width of the top, bottom and side plate respectively, d is the depth of the corrugation and c is the projection of the side plate width on the horizontal (see Fig. 2).

Referring to Fig. 5a, the forces acting on the corners of the corrugation are readily determined in terms of M_B and M_C and hence in terms of u_T, u_B and u_S as follows:

$$q_T = \frac{M_C}{b_T}, \tag{4}$$

$$q_B = -\frac{M_B}{b_B}, \tag{5}$$

$$q_S = \frac{M_C - M_B}{2b_S}. \tag{6}$$

Resolving forces at point B

$$p_B = -\frac{2b_S}{d} q_S - \frac{c}{d} q_B$$

or after substituting from Eqs. (5) and (6)

$$p_B = -\frac{1}{d}\left[M_C - \left(\frac{c}{b_B} + 1\right) M_B\right]. \tag{7}$$

Similarly

$$p_{SB} = q_B \frac{2b_S}{d} + q_S \frac{c}{d}$$

or

$$p_{SB} = -\frac{1}{d}\left[\left(\frac{2b_S}{b_B} + \frac{c}{2b_S}\right) M_B - \frac{c}{2b_S} M_C\right]. \tag{8}$$

Resolving forces at point C,

$$p_T = \frac{1}{d}\left[\left(1 + \frac{c}{b_T}\right) M_C - M_B\right] \tag{9}$$

and

$$p_{ST} = \frac{1}{d}\left[\left(\frac{2b_S}{b_T} + \frac{c}{2b_S}\right) M_C - \frac{c}{2b_S} M_B\right]. \tag{10}$$

Eqs. (8) and (10) together give

$$p_{ST} - p_{SB} = \frac{2b_S}{d}\left[\frac{M_C}{b_T} + \frac{M_B}{b_B}\right]. \tag{11}$$

Substituting from Eqs. (1) and (2) into (7), (9) and (11), one may obtain

$$2p_T = \frac{D}{d b_S^2 F}\left[K_{11} u_T + K_{12} u_B + K_{13} u_S\right], \tag{12}$$

$$2p_B = \frac{D}{d b_S^2 F}\left[K_{21} u_T + K_{22} u_B + K_{23} u_S\right], \tag{13}$$

$$p_{ST} - p_{SB} = \frac{D}{d b_S^2 F}\left[K_{31} u_T + K_{32} u_B + K_{33} u_S\right], \tag{14}$$

where

$$K_{11} = -2\left[(K+H_1)\left(1+\frac{c}{b_T}\right)+J-G_1\right],$$

$$K_{12} = 2\left[(K-H_1)\left(1+\frac{c}{b_T}\right)+J-G_1\right],$$

$$K_{13} = 2\left[H\left(1+\frac{c}{b_T}\right)-G\right],$$

$$K_{21} = 2\left[(J-G_1)\left(1+\frac{c}{b_B}\right)+K+H_1\right],$$

$$K_{22} = 2\left[-(J+G_1)\left(1+\frac{c}{b_B}\right)+K+H_1\right], \tag{15}$$

$$K_{23} = 2\left[G\left(1+\frac{c}{b_B}\right)-H\right],$$

$$K_{31} = 2\,b_S\left[\frac{H_1-K}{b_T}+\frac{J-G_1}{b_B}\right],$$

$$K_{32} = 2\,b_S\left[\frac{K+H_1}{b_T}-\frac{J+G_1}{b_B}\right],$$

$$K_{33} = 2\,b_S\left[\frac{H}{b_T}+\frac{G}{b_B}\right].$$

5. The Equilibrium of the Top, Bottom and Side Plates

Top Plate

Referring to Fig. 5b, an element of the top plate of length dy and width $2\,b_T$ is acted upon by forces:

a) $2\,p_T\,dy$ along $0\,X$;
b) shearing forces F_T and F_T+dF_T on either end of the element and two equal and opposite longitudinal forces $Q_T\,dy$;
c) beam type moments M_T and M_T+dM_T about axis $0\,Z$.

The following equilibrium conditions may be derived.

$$\frac{dF_T}{dy} = -2\,p_T, \tag{16}$$

$$\frac{dM_T}{dy} - 2\,b_T\,Q_T + F_T = 0. \tag{17}$$

With the in-plane deflection denoted by u_T, the moment-curvature rotation for the top plate is

$$\frac{E\,t\,(2\,b_T)^3}{12}\,\frac{d^2u_T}{dy^2} = M_T, \tag{18}$$

where $\frac{E t (2 b_T)^3}{12}$ is the flexural rigidity of the top plate about axis $0Z$. Differentiating Eq. (17) and substituting from (16) and (18),

$$\frac{2}{3} E t b_T^3 \frac{d^4 u_T}{dy^4} - 2 b_T \frac{d Q_T}{dy} - 2 p_T = 0. \tag{19}$$

Bottom Plate

With the forces applied on an element of the bottom plate as shown by Fig. 5b and proceeding as for the top plate, the equilibrium equation of the bottom plate may be written as:

$$\frac{2}{3} E t b_B^3 \frac{d^4 u_B}{dy^4} - 2 b_B \frac{dQ_B}{dy} - 2 p_B = 0. \tag{20}$$

Side Plate

Forces acting on an element of the side plate are as shown in Fig. 5b, giving the following equilibrium conditions.

$$\begin{aligned} &\frac{dF_S}{dy} = p_{ST} - p_{SB}, \\ &\frac{dM_S}{dy} + F_S - b_S (Q_T + Q_B) = 0, \\ &\frac{dP}{dy} + Q_T - Q_B = 0 \end{aligned} \tag{21}$$

and the moment-curvature relation

$$\frac{2}{3} E t b_S^3 \frac{d^2 u_S}{dy^2} = M_S.$$

Proceeding as before, the equilibrium equation for the side plate becomes

$$\frac{2}{3} E t b_S^3 \frac{d^4 u_S}{dy^4} - b_S \left(\frac{dQ_T}{dy} + \frac{dQ_B}{dy} \right) - (p_{ST} - {}_{SB}) = 0. \tag{22}$$

6. Compatibility of Deformations

Consider three points B, S, T on the mid-width of the bottom, side and top plate respectively as shown in Fig. 5b. If the three points had the same Y-coordinate before deformation, then after deformation let the relative shear displacement between B and T be

$$\Delta = 2 (\Delta_B + \Delta_T),$$

where Δ is the shear deformation per corrugation in the $0\,Y$ direction, Δ_B is the relative displacement between points S and B and Δ_T the relative displacement between points T and S.

The shear displacement across an element in the bottom plate, Fig. 5b, may be expressed as:

$$S_B = -2\,b_B \frac{du_B}{dy} + Q_B\,dy \frac{2\,b_B}{dy\,t\,N} = 2\left(-b_B \frac{du_B}{dy} + Q_B \frac{b_B}{t\,N}\right),$$

where $N = \dfrac{E}{2\,(1+\mu)}$ is the shear modulus of the plate.

Similarly for an element in the side plate,

$$S_S = -2\,b_S \frac{du_S}{dy} + Q_B\,dy \frac{b_S}{dy\,t\,N} + Q_T\,dy \frac{b_S}{t\,N} = -2\,b_S \frac{du_S}{dy} + \frac{b_S}{t\,N}(Q_T + Q_B)$$

and for an element in the top plate

$$S_T = 2\left(-b_T \frac{du_T}{dy} + Q_T \frac{b_T}{t\,N}\right).$$

Since, therefore,

$$\Delta = 2\,(\Delta_B + \Delta_T) = S_B + 2\,S_S + S_T$$

it follows that

$$\Delta = -2\,b_B \frac{du_B}{dy} - 4\,b_S \frac{du_S}{dy} - 2\,b_T \frac{du_T}{dy} + \frac{2\,Q_B}{t\,N}(b_B + b_S) + \frac{2\,Q_T}{t\,N}(_T + b_S). \quad (23)$$

Considering now longitudinal strain within the side plate, the strain at any point in direction $0_S\,Y_S$ due to normal force P, Fig. 5b, should equal the mean of the strains at either side of the width, $2\,b_S$, of the plate.

The strain at the top of the side plate is

$$\epsilon_T = -\frac{M_T\,b_T}{E\,I} = -b_T \frac{d^2\,u_T}{dy^2}.$$

Similarly

$$\epsilon_B = b_B \frac{d^2\,u_B}{dy^2},$$

whence

$$\frac{P}{2\,b_S\,t\,E} = \frac{1}{2}\left(-b_T \frac{d^2\,u_T}{dy^2} + b_B \frac{d^2\,u_B}{dy^2}\right)$$

or

$$P = -b_S\,t\,E\left(b_T \frac{d^2\,u_T}{dy^2} - b_B \frac{d^2\,u_B}{dy^2}\right). \quad (24)$$

7. The Simultaneous Differential Equations

The shear deflection per corrugation Δ is constant and independent of y, whence by differentiating Eq. (23),

$$\frac{dQ_B}{dy}(b_B + b_S) + \frac{dQ_T}{dy}(b_T + b_S) = t\,N\left(b_T \frac{d^2\,u_T}{dy^2} + 2\,b_S \frac{d^2\,u_S}{dy^2} + b_B \frac{d^2\,u_B}{dy^2}\right). \quad (25)$$

Differentiating (24) and substituting into (21),

$$Q_T - Q_B = -b_S t E\left(b_T \frac{d^3 u_T}{dy^3} - b_B \frac{d^3 u_B}{dy^3}\right). \tag{26}$$

Differentiating Eq. (26) and solving with Eq. (25) for $\frac{dQ_T}{dy}$ and $\frac{dQ_B}{dy}$,

$$\frac{dQ_T}{dy} = \frac{E t}{(b_T + 2 b_S + b_B)}\left[\frac{\phi}{2(1+\mu)} - b_S (b_B + b_S)\psi\right], \tag{27}$$

$$\frac{dQ_B}{dy} = \frac{E t}{(b_T + 2 b_S + b_B)}\left[\frac{\phi}{2(1+\mu)} + b_S (b_T + b_S)\psi\right] \tag{28}$$

and

$$\frac{dQ_T}{dy} + \frac{dQ_B}{dy} = \frac{E t}{(b_T + 2 b_S + b_B)}\left[\frac{\phi}{1+\mu} + b_S (b_T - b_B)\psi\right], \tag{29}$$

where

$$\begin{aligned} \phi &= b_T \frac{d^2 u_T}{dy^2} + 2 b_S \frac{d^2 u_S}{dy^2} + b_B \frac{d^2 u_B}{dy^2}, \\ \psi &= b_T \frac{d^4 u_T}{dy^4} = -b_B \frac{d^4 u_B}{dy^4}. \end{aligned} \tag{30}$$

Substituting from (27), (28), (29) and (30) and from Eqs. (12), (13) and (14) into Eqs. (19), (20) and (22), Eq. (19) becomes:

$$a_1 \frac{d^4 u_T}{dy^4} + a_2 \frac{d^2 u_T}{dy^2} + a_3 u_T + a_4 \frac{d^4 u_B}{dy^4} + a_5 \frac{d^2 u_B}{dy^2} + a_6 u_B + a_7 \frac{d^2 u_S}{dy^2} + a_8 u_S = 0, \tag{31}$$

Eq. (20) becomes

$$b_1 \frac{d^4 u_T}{dy^4} + b_2 \frac{d^2 u_T}{dy^2} + b_3 u_T + b_4 \frac{d^4 u_B}{dy^4} + b_5 \frac{d^2 u_B}{dy^2} + b_6 u_B + b_7 \frac{d^2 u_S}{dy^2} + b_8 u_S = 0 \tag{32}$$

and Eq. (21) becomes:

$$\begin{aligned} c_1 \frac{d^4 u_T}{dy^4} + c_2 \frac{d^2 u_T}{dy^2} + c_3 u_T + c_4 \frac{d^4 u_B}{dy^4} + c_5 \frac{d^2 u_B}{dy^2} + c_6 u_B \\ + c_7 \frac{d^4 u_S}{dy^4} + c_8 \frac{d^2 u_S}{dy^2} + c_9 u_S = 0, \end{aligned} \tag{33}$$

where

$$\begin{aligned} a_1 &= A b_T^3 + 2 B b_T^2 b_S (1+\mu)(b_B + b_S), \\ a_2 &= -B b_T^2, \\ a_3 &= -K_{11}, \\ a_4 &= -2 B b_S b_T b_S (1+\mu)(b_B + b_S), \\ a_5 &= -B b_T b_B, \\ a_6 &= -K_{12}, \\ a_7 &= -2 B b_S b_T, \\ a_8 &= -K_{13}, \\ b_1 &= -2 B b_S b_B b_T (1+\mu)(b_T + b_S), \end{aligned} \tag{34}$$

$$
\begin{aligned}
b_2 &= -B b_B b_T, \\
b_3 &= -K_{21}, \\
b_4 &= A b_B^3 + 2 B b_S b_B^2 (1+\mu)(b_T + b_S), \\
b_5 &= -B b_B^2, \\
b_6 &= -K_{22}, \\
b_7 &= -2 B b_B b_S, \\
b_8 &= -K_{23}, \\
c_1 &= -B b_S^2 b_T (1+\mu)(b_T - b_B), \\
c_2 &= -B b_S b_T, \\
c_3 &= -K_{31}, \\
c_4 &= B b_S^2 b_B (1+\mu)(b_T - b_B), \\
c_5 &= -B b_S b_B, \\
c_6 &= -K_{32}, \\
c_7 &= A b_S^3, \\
c_8 &= -2 B b_S^2, \\
c_9 &= -K_{33}, \\
A &= 8 \left(\frac{b_S}{t}\right)^2 dF (1-\mu^2), \\
B &= \frac{12 \left(\frac{b_S}{t}\right)^2 dF (1-\mu)}{(b_T + 2 b_S + b_B)}.
\end{aligned}
\tag{34}
$$

Eqs. (31), (32) and (33) are the equilibrium equations of a corrugated plate shear panel. The equations are simultaneous differential equations of the fourth order, thus twelve boundary conditions are needed for the solution. An exact solution for the equations not being available, a numerical method using finite differences [8, 9] has been used.

8. The Boundary Conditions

The boundary conditions follow from the anti-symmetry of deformation of the panel about the mid-length and from the assumptions made under 3., and are as follows.

a) At the Mid-length of the Panel:

$$(u_T)_{y=0} = 0, \tag{35}$$

$$(u_B)_{y=0} = 0, \tag{36}$$

$$(u_S)_{y=0} = 0, \tag{37}$$

$$(M_T)_{y=0} = (M_B)_{y=0} = (M_T)_{y=0} = 0$$

or
$$\left(\frac{d^2 u_T}{dy^2}\right)_{y=0} = 0, \tag{38}$$
$$\left(\frac{d^2 u_B}{dy^2}\right)_{y=0} = 0, \tag{39}$$
$$\left(\frac{d^2 u_S}{dy^2}\right)_{y=0} = 0. \tag{40}$$

b) At the End of the Panel:

$$(u_B)_{y=a} = 0, \tag{41}$$
$$(u_S)_{y=a} = 0, \tag{42}$$
$$(M_T)_{y=a} = (M_B)_{y=a} = (M_S)_{y=a} = 0$$

or
$$\left(\frac{d^2 u_T}{dy^2}\right)_{y=a} = 0, \tag{43}$$
$$\left(\frac{d^2 u_B}{dy^2}\right)_{y=a} = 0, \tag{44}$$
$$\left(\frac{d^2 u_S}{dy^2}\right)_{y=a} = 0 \tag{45}$$

and lastly $(F_T)_{y=a} = 0$ (a)

or $(F_B + 2 F_S \sin\theta)_{y=a} = R.$ (b)

From 5., by the integration of Eqs. (20) and (22),

$$F_B = 2 b_B Q_B - \frac{2}{3} E t b_B^3 \frac{d^3 u_B}{dy^3} \tag{c}$$

and
$$F_S = b_S (Q_T + Q_B) - \frac{2}{3} E t b_S^3 \frac{d^3 u_S}{dy^3}. \tag{d}$$

Substituting from (a) into (17),

$$2 b_T (Q_T)_{y=a} = \frac{2}{3} E t b_T^3 \left(\frac{d^3 u_T}{dy^3}\right)_{y=a}. \tag{e}$$

Eqs. (21) and (24) give:

$$Q_T - Q_B = b_S t E \left(b_T \frac{d^3 u_T}{dy^3} - b_B \frac{d^3 u_B}{dy^3}\right). \tag{f}$$

By substituting from (e) into (f) and then for $(Q_T)_{y=a}$ and $(Q_B)_{y=a}$ into (c) and (d) and hence into Eq. (b) we finally obtain

$$d_1 \left(\frac{d^3 u_T}{dy^3}\right)_{y=a} + d_2 \left(\frac{d^3 u_B}{dy^3}\right)_{y=a} + d_3 \left(\frac{d^3 u_S}{dy^3}\right)_{y=a} = \frac{R}{E t}, \tag{46}$$

where

$$d_1 = 2b_B\left(\frac{b_T^2}{3} - b_S b_T\right) + c\left(\frac{2}{3}b_T^2 - b_S b_T\right),$$

$$d_2 = 2b_S b_B^2 - \frac{2}{3}b_B^3 + b_S b_B c, \tag{47}$$

$$d_3 = -\frac{2}{3}b_S^2 c.$$

The solution of Eqs. (31), (32) and (33), subjected to the boundary conditions of Eqs. (35) through (47), by the central difference method, follows standard procedures. It is described in detail in reference [8].

9. Solved Examples

Figs. 6 to 10 show the results obtained by the above analysis for the given corrugation configurations of various lengths.

As shown by the energy solution [1], the length of a panel has major effects on its shear behaviour. It is thus convenient to discuss the behaviour of the panel under consideration according to three different groups depending on its length: a) short panels, b) medium length panels and c) long panels.

a) Short Panels

Fig. 6 shows that, for a short length panel ($a < 50$ ins. in the example), the top plate deflection u_T is almost a straight line. The bottom plate deflection

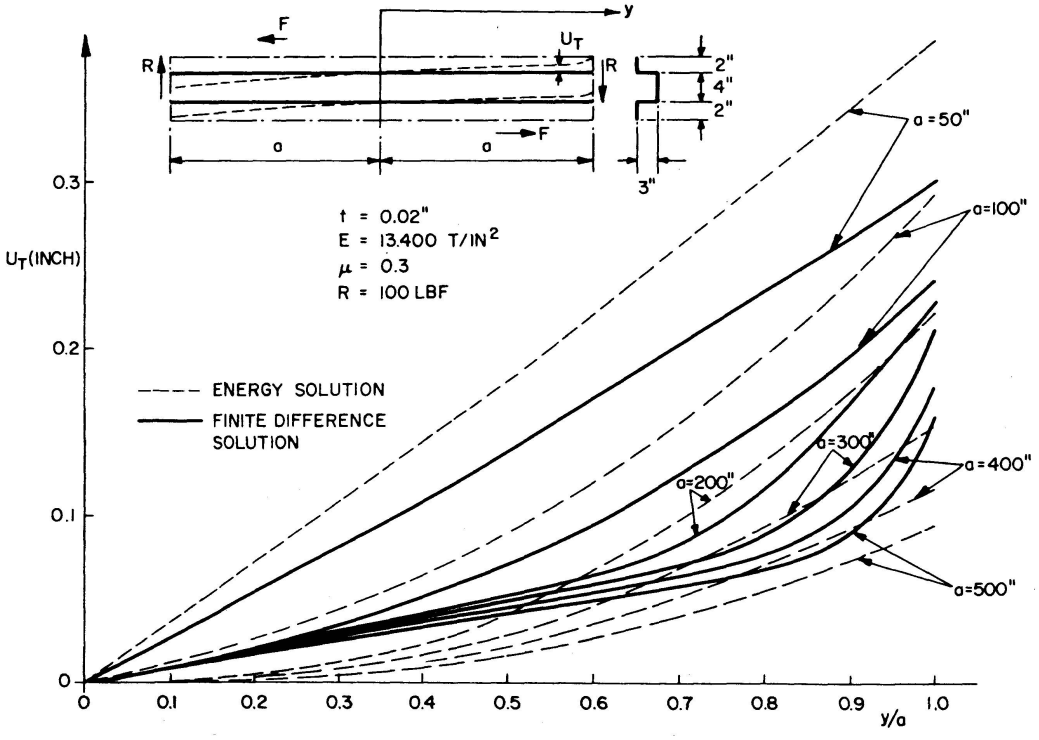

Fig. 6.

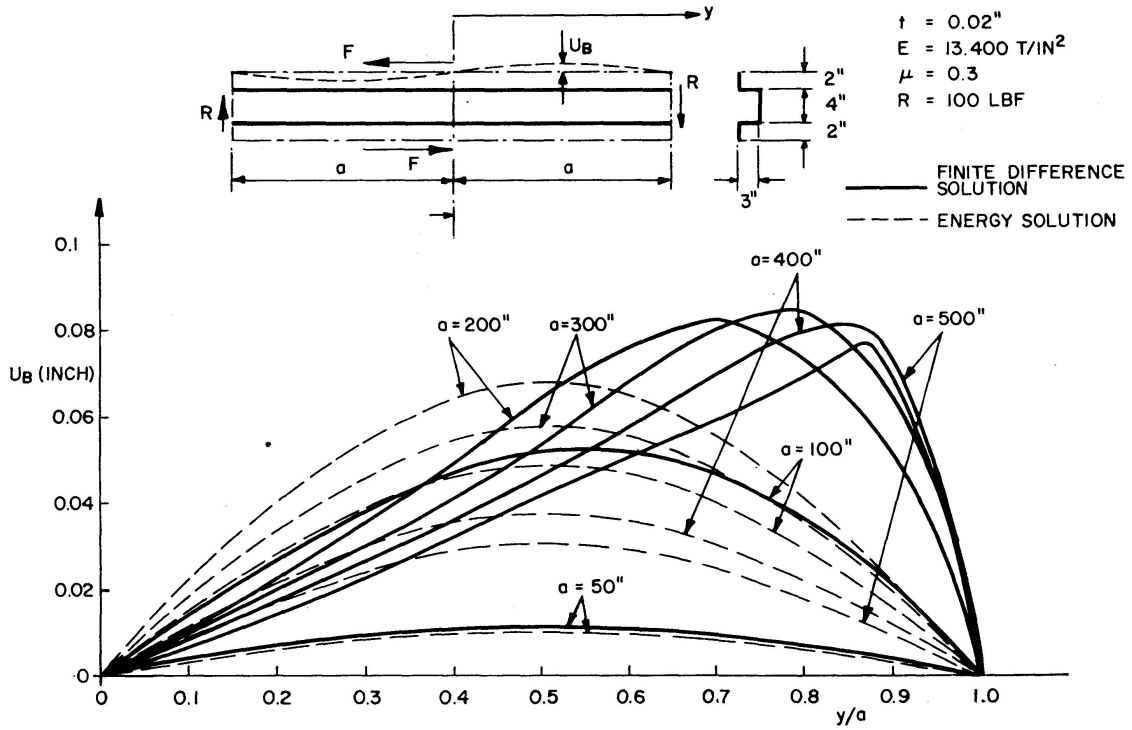
y
F
U_B
R
R
a
F
a
2"
4"
2"
3"
t = 0.02"
E = 13.400 T/IN²
μ = 0.3
R = 100 LBF
FINITE DIFFERENCE SOLUTION
ENERGY SOLUTION
U_B (INCH)
0.1
0.08
0.06
0.04
0.02
0
a=400"
a=200"
a=300"
a=500"
a=100"
a=50"
0 0.1 0.2 0.3 0.4 0.5 0.6 0.7 0.8 0.9 1.0
y/a

Fig. 7.

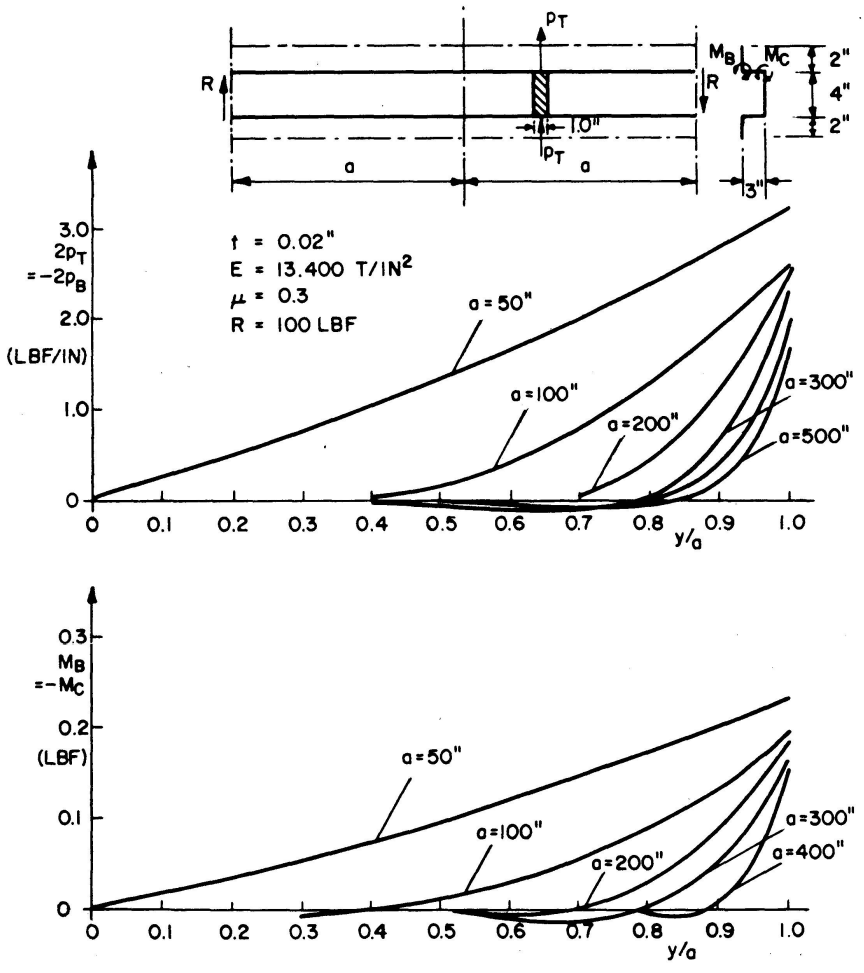
p_T
R
R
M_B
M_C
2"
4"
2"
1.0"
p_T
a
a
3"
t = 0.02"
E = 13.400 T/IN²
μ = 0.3
R = 100 LBF
3.0
$2p_T$
$=-2p_B$
2.0
(LBF/IN)
1.0
0
a=50"
a=100"
a=200"
a=300"
a=500"
0 0.1 0.2 0.3 0.4 0.5 0.6 0.7 0.8 0.9 1.0
y/a
0.3
M_B
$=-M_C$
0.2
(LBF)
0.1
0
a=50"
a=100"
a=200"
a=300"
a=400"
0 0.1 0.2 0.3 0.4 0.5 0.6 0.7 0.8 0.9 1.0
y/a

Fig. 8.

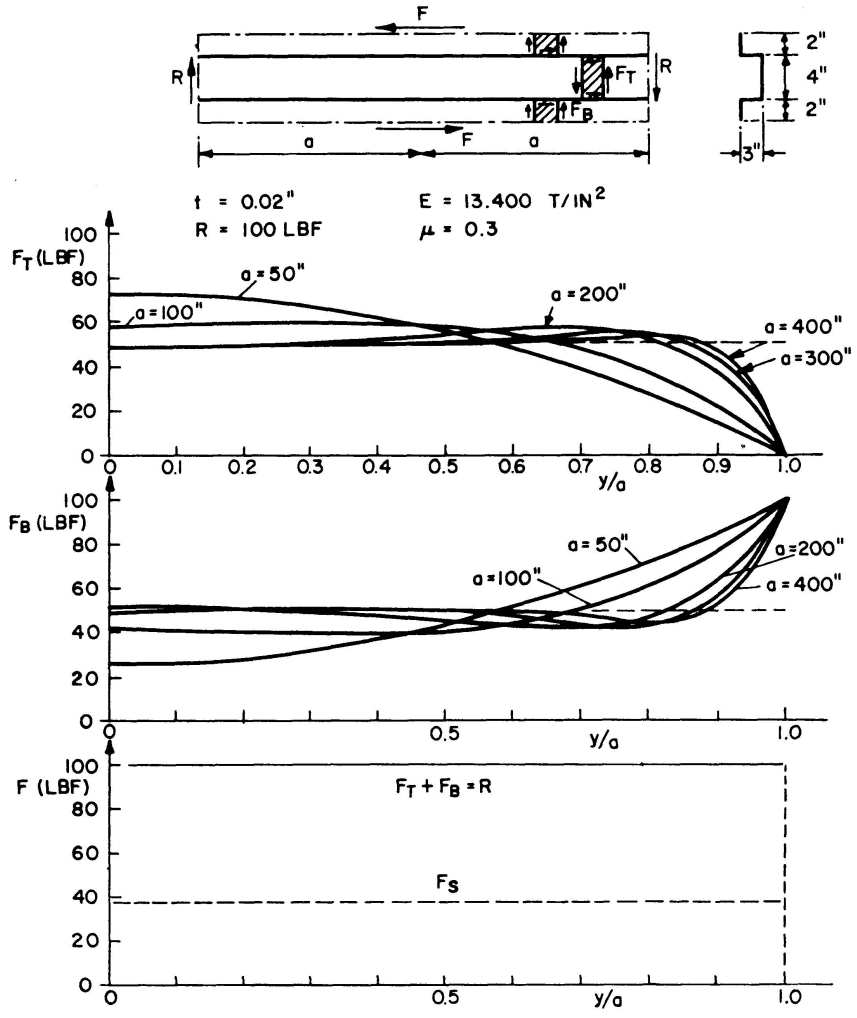

Fig. 9.

u_B, Fig. 7, and the side plate deflection u_S are very small compared with u_T and consequently have small effects on the panel behaviour. Therefore, for panels in this "short" category, the top, bottom and side plates may be treated as infinitely rigid, with deflections

$$u_T = k\,y,$$
$$u_B = u_S = 0,$$

where k is a constant. Hence from Eqs. (1) and (2), the portal frame moments M_B and M_C vary linearly along 0 Y (Fig. 8). Similarly, from Eqs. (12), (13) and (14), p_T, p_B and $p_{ST} - p_{SB}$ also vary linearly with y. From Eq. (16), since $(F_T)_{y=a} = 0$, we have

$$F_T = \frac{k_1}{2}(y^2 - a^2),$$

where k_1 is a constant. The shear forces in the bottom plate (F_B) are also distributed parabolically, but with the maximum value at the ends. The

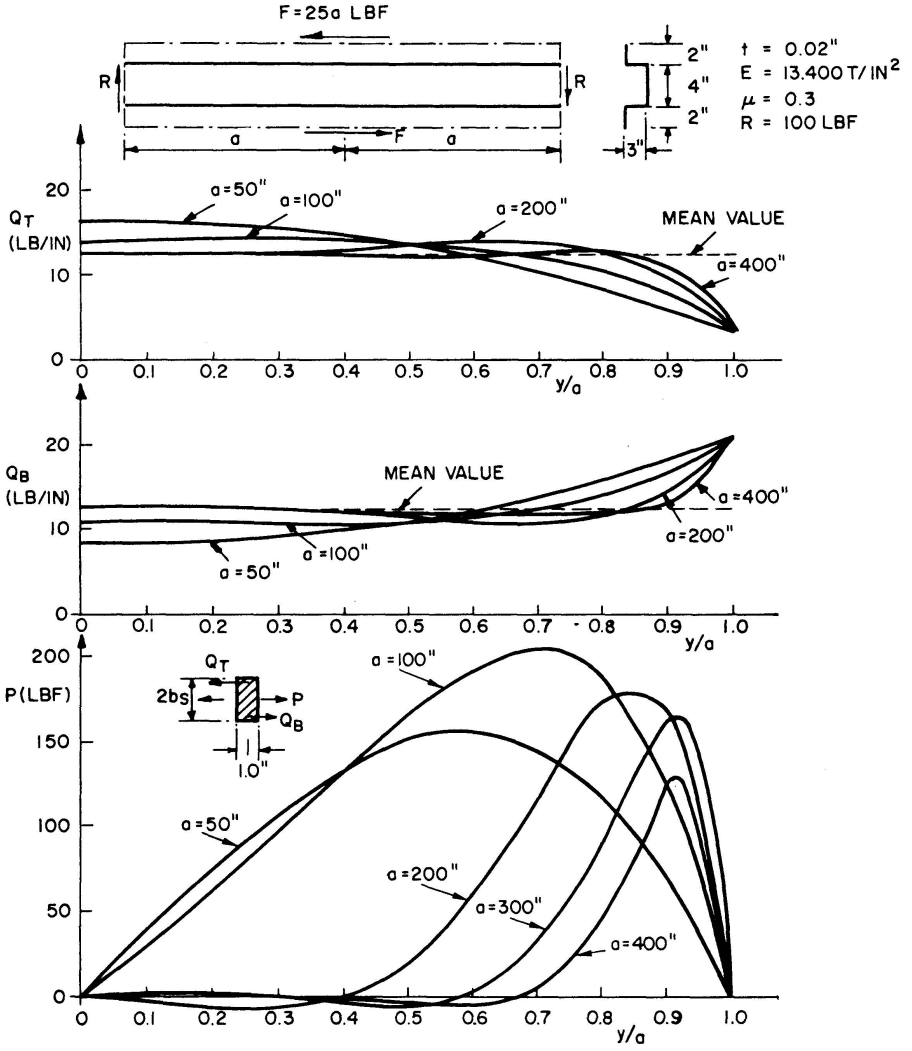

Fig. 10.

distribution of F_T and F_S is shown in Fig. 9a and b. The sum of the shear forces $F_T + F_B$ ($\sin\theta = 0$ in the example) is constant at any point and equal to the external applied force ($R = 100$ lbf) as shown by Fig. 9c.

Since the shear forces F_T and F_B are related to the shear forces per unit length Q_T and Q_B, the later will also have parabolic distributions along the panel length as shown in Fig. 10.

b) Medium Length Panels

As the length of the panel increases, significant "beam" bending stresses develop in the top, bottom and side plates. The top plate deflection u_T becomes curved (Fig. 6) and the bottom and side plate deflections u_B and u_S increase (Fig. 7).

The shear forces F_T and F_B (Fig. 9) and Q_T and Q_B (Fig. 10) become more uniform in value over the middle length of the panel and only change significantly near the ends.

c) Long Panels

When the panel becomes longer (more than 200 ins. in the example), "beam" bending in the plates becomes concentrated at the ends (Fig. 11). It is seen from Figs. 8, 9 and 10 that all the internal forces become almost uniform over the central length of the panel. These uniform values are given closely by

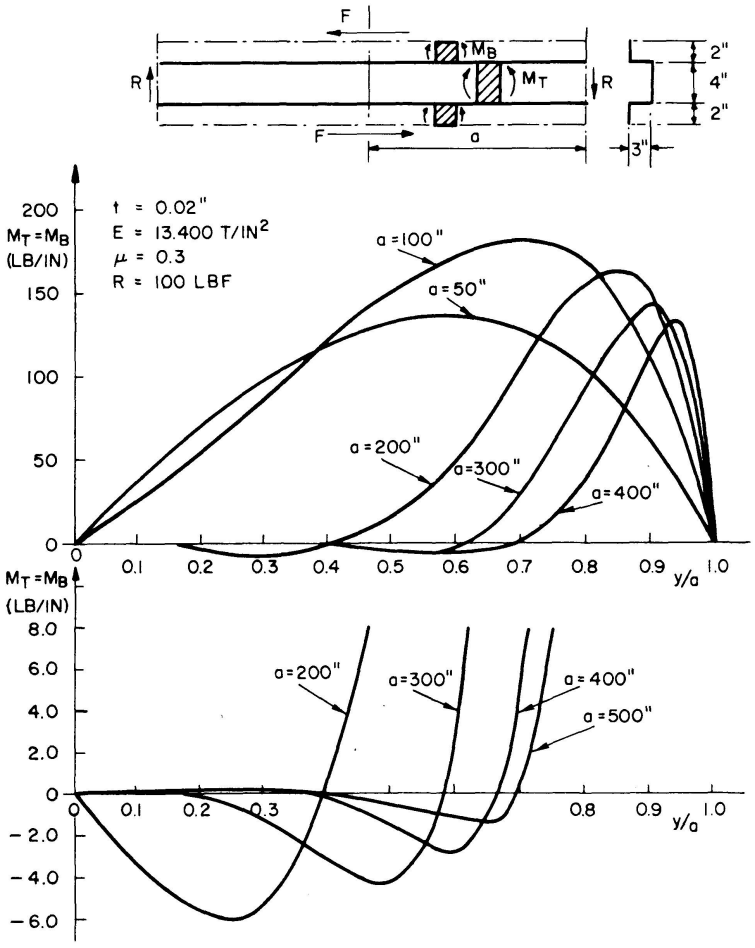

Fig. 11.

$$F_T = \frac{R\,b_T}{(b_T + b_B + 2\,b_S \sin\theta)},$$

$$F_B = \frac{R\,b_B}{(b_T + b_B + 2\,b_S \sin\theta)},$$

$$F_S = \frac{R\,b_S}{(b_T + b_B + 2\,b_S \sin\theta)},$$

$$Q_T = Q_B = \frac{R}{2\,(b_T + b_B + 2\,b_S \sin\theta)}.$$

The deflections of the top and bottom side plates (Figs. 6 and 7) vary almost linearly except near the ends of the panel, where the deflection of the top plate

increases more rapidly, while that of the bottom plate suddenly decreases to zero. It is seen that this behaviour is not revealed by the energy method also presented by the authors [1].

A comparison between theoretical and experimental results is given in Table 1. It is seen that there is good agreement between test results and the method presented in the paper. The energy method gives less consistently good results, but is still likely to be sufficiently accurate for practical purposes.

Table 1

Reference	Details of Panel	Shear Flexibility, in tonf		
		Test Result	Theoretical Energy Method	Theoret. Finite Differ. Method
2 (Type 1 sheeting – 3 purlins)	$2b_T$ = 4.125 in $2b_B$ = 1.375 in d = 1.375 in c = 0.625 in $2a$ = 144 in Et^3 = 2.95 tonf-in	0.056	0.044	0.055
2 (Type 2 sheeting – 3 purlins)	$2b_T$ = 4.625 in $2b_B$ = 1.75 in d = 2.53 in c = 0.8125 in $2a$ = 144 in Et^3 = 2.95 tonf-in	0.134	0.146	0.133
4	$2b_T$ = 4.73 in $2b_B$ = 2.76 in d = 3.54 in c = 0.59 in $2a$ = 78.8 in Et^3 = 142 tonf-in	0.40×10^{-3}	0.42×10^{-3}	0.44×10^{-3}

References

1. Horne, M. R. and Raslan, R. A.: "An energy solution to the shear deformation of corrugated plates" (see above).
2. Bryan, E. R. and El-Dakhakhni, W. M.: "Shear of corrugated decks: calculated and observed behaviour." Proc. Instn. Civ. Engrs., Vol. 41, Nov. 1968.
3. Bryan, E. R. and El-Dakhakhni, W. M.: "Shear flexibility and strength of corrugated decks." Proc. Am. Soc. Civ. Engrs. Str. Div., Nov. 1968.
4. Bryan, E. R. and Jackson, P.: "The shear behaviour of corrugated steel sheeting." Thin-walled Structures Symposium, University of Swansea, 1967.
5. Falkenberg, J. C.: Discussion on "Shear flexibility and strength of corrugated decks." Journal of Str. Div., Proc. Am. Soc. Civ. Engrs., June, 1969.
6. Luttrell, L. D.: "Structural performance of light gauge steel diaphragms." Report No. 319, Dept. of Structural Engineering, Cornell University, 1965.

7. McKenzie, K. I.: "The shear stiffness of a corrugated web." Aeronautical Research Council Reports and Memoranda No. 3342, London, 1963.
8. Raslan, R. A. S.: "The structural behaviour of corrugated plates." Ph. D. Thesis, University of Manchester, 1969.
9. Fox, L.: "The Numerical Solution of Two-Point Boundary Problems in Ordinary Differential Equations." Oxford University Press, 1957.

Summary

The shear behaviour of a panel with trapezoidal corrugations is investigated by setting up the differential equations for the bending in their own planes of the top, bottom and side plates of the corrugations, treating them as prismatic beams. A numerical solution is then achieved, using finite difference. The behaviour is found to depend on the length of the panel, measured parallel to the corrugations. The predicted shear flexibilities of some panels for which test results are available are found to agree well with the experimental values.

Résumé

Le comportement d'un champ à raidisseurs trapézoidale est étudié à l'aide des équations différentielles de la flexion dans leurs propres plans, c.-à-d. des tôles supérieures, inférieures et latérales des raidisseurs, en considérant celles-ci comme des poutres prismatiques. Une solution numérique est finalement atteinte par l'utilisation des différences finies. On trouve que le comportement dépend de la longueur du champ mesurée parallèlement aux raidisseurs. Les déformations dues au cisaillement prévues pour certains champs, pour lesquels des essais ont été entrepris, correspondent très bien avec les valeurs expérimentales.

Zusammenfassung

Das Schubverhalten eines Feldes mit trapezförmigen Rippen wird durch Aufstellen der Differentialgleichungen für das Biegen in ihrer eigenen Ebene der oberen, unteren und seitlichen Bleche der Rippen untersucht, indem diese als prismatische Träger behandelt werden. Eine numerische Lösung ergibt sich dann unter Benützung endlicher Differenzen. Man findet, dass das Verhalten von der Länge des Feldes, gemessen parallel zu den Rippen abhängt. Die vorausgesagten Schubbiegsamkeiten einiger Felder, für die Versuchsresultate greifbar waren, ergaben sich als gut übereinstimmend mit den experimentellen Werten.